

A neutron diffraction study of deuterium short-range order in $\text{VD}_{0.75}$

This article has been downloaded from IOPscience. Please scroll down to see the full text article.

1994 J. Phys.: Condens. Matter 6 1461

(<http://iopscience.iop.org/0953-8984/6/8/005>)

View [the table of contents for this issue](#), or go to the [journal homepage](#) for more

Download details:

IP Address: 171.66.16.147

The article was downloaded on 12/05/2010 at 17:41

Please note that [terms and conditions apply](#).

A neutron diffraction study of deuterium short-range order in $\text{VD}_{0.75}$

U Knell†, H Wipf†, G Lautenschläger‡, R Hock‡, H Weitzel‡ and E Ressouche§

† Institut für Festkörperphysik, Technische Hochschule Darmstadt, Hochschulstraße 6, D-64289 Darmstadt, Germany

‡ Fachbereich Materialwissenschaften, Technische Hochschule Darmstadt, Petersenstraße 20, D-64287 Darmstadt, Germany

§ DRFMC/MDN, Centre d'Etude Nucleaire de Grenoble, 17 Avenue des Martyrs, F-38041 Grenoble, France

Received 28 June 1993, in final form 7 September 1993

Abstract. We investigated the short-range order of D interstitials in cubic (α' -phase) $\text{VD}_{0.75}$ by neutron diffraction (room temperature measurements, powder sample). The VD_x system is particularly favourable for neutron scattering experiments studying the short-range order of hydrogen interstitials in metals since the coherent scattering cross section of D exceeds the coherent cross section of V by a factor of ≈ 300 . This allows a data analysis that assumes that only the D atoms contribute to the coherent scattering intensity. The measured diffuse scattering intensity shows a nearly complete blocking of interstitial sites in the two nearest shells around a given D atom, and a reduced occupation probability for the sites in the third shell. The results indicate the existence of a strong short-range and repulsive interaction between the D atoms.

1. Introduction

H interstitials in BCC metals such as V, Nb or Ta occupy tetrahedral sites, at least in the cubic (α or α') phases of the respective metal–hydrogen system [1]. An important characteristic of these systems is the small distances between two nearest neighbour sites. The distances only slightly exceed 1 Å, thus being almost a factor of two smaller than the shortest distance between the octahedral interstitial sites of the H in FCC metals such as Pd [2]. A consequence of the small distances between interstitial sites in BCC metals is that tunnelling is an effective mechanism for H diffusion [3]. A second important consequence is that we can expect distinct short-range order effects between the H interstitials. In fact, band structure calculations [4, 5] and the structure of the non-cubic hydride phases [6] suggest a repulsive short-range interaction between the H, suppressing any significant occupation of interstitial sites in the nearest [5] or the two nearest [4, 6] shells around a given H atom. The suggestion is in line with the results of solubility measurements [7, 8] in the cubic α or α' phases, which show an extremely steep rise of the chemical potential of the H for H–metal atom ratios x close to about 0.8 although a full occupation of all tetrahedral interstitial sites corresponds to $x = 6$. This behaviour of the chemical potential agrees with a short-range repulsive interaction, and a great number of theoretical calculations for the thermodynamic properties of H in BCC metals have been successfully carried out under the assumption that a H atom blocks completely, or nearly completely, the interstitial sites in the two or even three nearest-neighbour shells [9–13]. Finally the results of a recent neutron scattering study

[14], carried out on the system NbD_x , indicate also a complete blocking of the first and second shells.

The analyses mentioned above show the existence of a strong and repulsive short-range interaction between H atoms in BCC metals. The most immediate information on these interaction effects is likely to be derived from diffuse neutron scattering studies [15, 16] such as that carried out on NbD_x [14] (x-ray scattering will not directly detect short-range order effects between the H atoms because of their small scattering cross section). In this paper, we report the results of diffuse neutron scattering measurements on the deuterated system VD_x ($x = 0.75$) in which we study short-range order between the D atoms. Our results prove the existence of a distinct short-range order, characterized by a (within experimental accuracy) complete blocking of the interstitial sites in the first shell around a D atom, and by a strongly reduced occupation of the sites in the second shell.

The system VD_x was selected for the present study for two reasons. Firstly, and most importantly, the coherent scattering cross section of D exceeds the coherent cross section of V by a factor of ≈ 300 [17]. This means that the coherent scattering intensity of our samples can be described completely by the scattering of the D atoms. Secondly, the cubic α' phase of the VD_x system exists at room temperature in the high concentration range between $x \approx 0.71$ and 0.88 [1]. This is a specific behaviour of the VD_x system which allows diffuse neutron scattering measurements to be carried out at both low temperatures and high D concentrations where short-range order effects are particularly strong. These favourable conditions also motivated a previous neutron scattering study although this did not provide meaningful conclusions on short-range order effects of D in V [18].

2. Samples and experimental details

Our measurements were performed at room temperature ($T \approx 295$ K) on a $\text{VD}_{0.75}$ powder sample (mean particle size ≈ 30 μm , maximum particle size < 90 μm , powder density ≈ 0.5) and on a D free reference sample with the same V content. Both samples were enclosed in Al containers with a diameter of 1 cm. Due to this sample dimension, multiple scattering represented $\approx 13\%$ of the total scattering intensity [19]. This fact allowed the neglect of multiple-scattering events in our data analysis, in particular under consideration of the fact that necessary model assumptions such as those on the scattering from the static displacements of the D atoms (see section 4) have a higher and more direct impact on the diffraction pattern and especially on its dependence on the neutron momentum transfer. The neutron data were obtained with the powder diffractometer DN5 at the Siloe reactor of the CENG. The diffractometer DN5 has a multicounter consisting of 800 cells with an angular distance of 0.1° (it is almost identical to the instrument D1B of the ILL [20]). The wavelength of the incident neutrons was $\lambda = 1.349$ \AA , corresponding to an energy of 44.94 meV. The collimation before the monochromator was $30'$.

The diffractometer used in the present experiments allows the investigation of a larger range of momentum transfer than the time of flight spectrometer IN5 (ILL) [20] used in the previous neutron study on D short-range order in NbD_x [14]. Furthermore, it provides a higher momentum resolution and count rate. The advantage of the time of flight spectrometer is its energy analysis, which permits an experimental separation of the inelastic scattering from the phonons. Since the inelastic scattering intensity is larger at higher temperature, an experimental separation of this inelastic intensity was important in the experiments on NbD_x [14], carried out at temperatures up to 581 K. For NbD_x , the experimental separation of the inelastic intensity was of further importance because of the significant coherent

inelastic (and elastic) background scattering from Nb–D and Nb–Nb correlations, which is undesired since it does not directly yield information on the D short-range order although it exhibits a distinct modulation with the momentum transfer of the neutrons (the Nb–Nb correlations contribute to the diffuse scattering intensity because of the lattice displacements resulting from the D interstitials; see section 4). On the other hand, the lower temperature of the present measurements and the fact that, for VD_x , a coherent scattering intensity from V–D correlations does not practically exist makes it perfectly possible to perform these measurements without an experimental separation of the inelastic scattering intensity (see discussion in sections 4 and 5).

3. Experimental results

Figure 1 presents the powder diffractogram of the $VD_{0.75}$ sample (top diffractogram) together with the diffractogram of the D free reference sample (bottom diffractogram). Both the sample investigated and the Al container produced Bragg reflections, which are specified in detail in the figure caption. The Bragg reflections in figure 1 demonstrate that the lattice parameter of the $VD_{0.75}$ sample is almost 5% larger than that of the reference sample [21]. The figure also shows that the intensities of the Bragg reflections of the Al container differ greatly between the two spectra as a consequence of the texture of the container material.

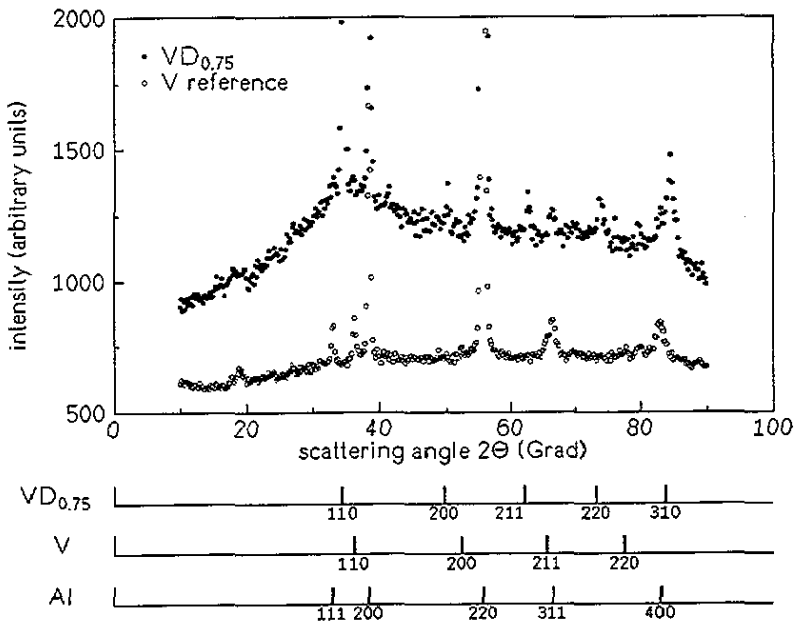


Figure 1. Powder spectrum of the $VD_{0.75}$ sample (full data points) and of the D free reference sample with the same V content (open data points). The bars below the spectra indicate the position of the Bragg peaks of the $VD_{0.75}$ sample, of the V reference and of Al (the main alloy component of the container). Several smaller peaks are caused by other alloy components of the container material.

The diffuse scattering intensity between the Bragg reflections of the $VD_{0.75}$ sample in figure 1 reflects the short-range order of the D atoms. Therefore, and in order to analyse

quantitatively the short-range order effects, we shall concentrate our subsequent discussion on the diffuse scattering intensity. Figure 2 presents a difference spectrum between the two spectra in figure 1, where the intensity of the D free reference sample is subtracted from that of the $VD_{0.75}$ sample. To simplify the analysis further, the intensity in the close neighbourhood of the Bragg reflections of both sample and container was omitted in the difference spectrum of figure 2.

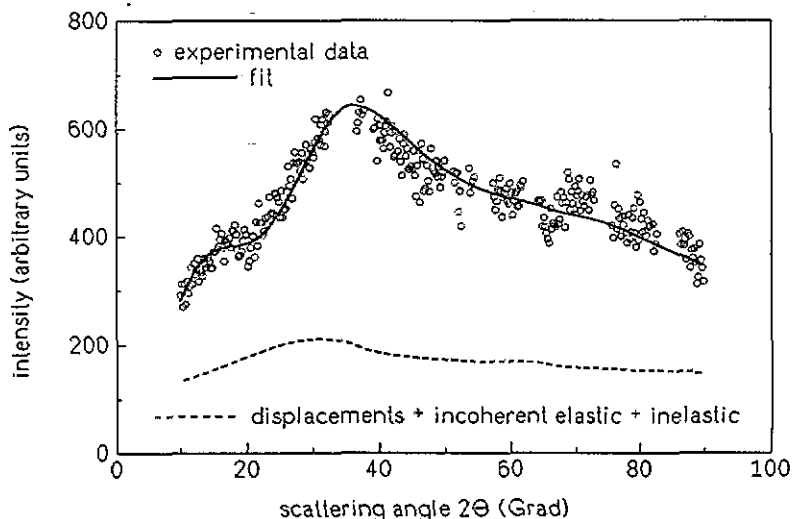


Figure 2. Diffuse scattering intensity of the D atoms in $VD_{0.75}$. The spectrum shows the difference between the spectra in figure 1, omitting the intensity in the close neighbourhood of the Bragg reflections. The solid line is a fit to the data with occupation probabilities c_j as mentioned in section 5 and table 1. The broken line shows the sum of the diffuse scattering intensities specified by (ii), (iii), (iv) and (v) in section 4 (scattering from the displacements of the D atoms, incoherent elastic scattering and the inelastic scattering from the optic and acoustic D vibrations).

4. Theoretical background

Because of the extremely small coherent scattering cross section of V, we need only account for incoherent scattering events from the V atoms. It is further well justified to assume that the V vibrations in the VD_x samples and the reference sample are so similar that the resulting diffuse incoherent inelastic scattering intensity is practically identical for all our samples. This means that the difference spectra in figures 2 and 3 represent solely the coherent and the incoherent diffuse scattering intensity from the D atoms in the $VD_{0.75}$ sample. For this diffuse scattering intensity, we expect five different contributions as follows:

- (i) the coherent elastic scattering from the D short-range order;
- (ii) the coherent elastic scattering from static displacements of the D atoms;
- (iii) the incoherent elastic scattering;
- (iv) the coherent and incoherent inelastic scattering from the optic D vibrations (local modes) and
- (v) the coherent and incoherent inelastic scattering from the acoustic D vibrations (band modes).

In the following, we shall quantitatively discuss the above contributions to the scattering intensity. A point to mention straight away is that each of the contributions (ii)–(v) will turn out to be much smaller than the short-range order contribution (i), and that even the of the contributions (ii)–(iv) is smaller than the contribution (i). This is important since it allows the use of simplifying approximations for some of the contributions (ii)–(v) without seriously impairing the reliability of our results.

4.1. Coherent elastic scattering from the D short-range order

For our present powder samples, the scattering cross section $(d\sigma/d\Omega)_{\text{SRO}}$ per D atom resulting from the coherent elastic short-range order contribution (i) can be written as [15, 16]

$$\left(\frac{d\sigma}{d\Omega}\right)_{\text{SRO}} = \frac{\sigma_{\text{coh}}}{4\pi} e^{-2W(Q)} \left\{ 1 - c + \sum_{j=1}^{\infty} N_j (c_j - c) \frac{\sin(QR_j)}{QR_j} \right\} \quad (1)$$

where $\sigma_{\text{coh}} = 5.59b$ [17] is the coherent scattering cross section of the D, $e^{-2W(Q)}$ is the Debye–Waller factor of the D, and $c = x/6 = 0.125$ is the occupation probability of an tetrahedral interstitial site (there are six tetrahedral sites per V host lattice atom). The quantity $Q = k_i - k_f$ is the difference between the wave vector k_i of the incident neutrons and the wave vector k_f of the scattered neutrons. The scattering angle 2Θ and $Q = |Q|$ are related according to

$$Q = \sqrt{k_i^2 + k_f^2 - 2k_i k_f \cos(2\Theta)} \quad (2)$$

where the relation $k_f = k_i$ holds for elastic scattering processes such as those described by equation (1). The summation in equation (1) extends over all shells of tetrahedral interstitial sites around a given tetrahedral site in the centre of the shells, where R_j is the distance between the site in the centre and the sites in shell j and N_j is the number of the sites in shell j . The quantity c_j is the probability that an interstitial site in shell j is occupied, provided that the tetrahedral site in the centre of the shell is also occupied. The correlation probabilities c_j describe, accordingly, the short-range order between the D atoms.

The calculation of the scattering cross section $(d\sigma/d\Omega)_{\text{SRO}}$ for given values of the correlation probabilities c_j requires the knowledge of the Debye–Waller factor $e^{-2W(Q)}$. The quantitative determination of this quantity from data in the literature will be discussed in section 4.6.

In this paper, the D correlations are described with the help of the probabilities c_j as defined above. In the literature, short-range order effects are frequently described with a parameter $\epsilon(R_j)$ [15] or, alternatively, with the so-called Cowley–Warren parameters α_j [16]. In the present situation, the relation between c_j , $\epsilon(R_j)$ and α_j is given by

$$c_j - c = \epsilon(R_j)/c = \alpha_j(1 - c). \quad (3)$$

4.2. Coherent elastic scattering from the static displacements of the D atoms

The D interstitials cause static lattice distortions, which lead to a displacement of the positions of the surrounding D atoms. The displacements yield a contribution to the total scattering intensity [15, 16, 22]. In the following, we shall calculate the scattering cross section $(d\sigma/d\Omega)_{\text{dis}}$ per D atom due to the displacements of these atoms under simplifying assumptions. The assumptions are justified by the fact that the contribution of the static

displacements to the scattering intensity is much smaller than the contribution from short-range order. We mention also that the present situation differs from that of previous studies on metal-H systems where H induced displacements of the host metal atoms were investigated by neutron or x-ray scattering [23, 24]. The difference follows from the fact that the displacements of the metal atoms are much larger than the displacements of the H atoms because of the larger distances between neighbouring H atoms in the presence of blocking effects.

The calculation of $(d\sigma/d\Omega)_{\text{dis}}$ requires the knowledge of the displacement $u(R)$ of a given D atom due to a second D atom at a distance R . We calculate $u(R)$ with the help of elasticity theory, assuming elastic isotropy. In this case, the displacement vector $u(R)$ is parallel to the vector R , and the value of $u(R)$ is, for an infinitely large crystal, given by [15, 25]

$$u(R) = \frac{1 + \sigma}{3(1 - \sigma)} \frac{\Delta V}{4\pi R^2} \quad (4)$$

where ΔV is the volume increase due to a D atom and σ is Poisson's ratio. The value of ΔV is 2.6 \AA^3 [21], whereas the factor $(1 + \sigma)/[3(1 - \sigma)]$ is found to be 0.7 after an orientational averaging of the elastic moduli of V [26]. Neglecting higher than two-particle correlation effects for the D atoms, under consideration of the fact that the displacements $u(R)$ are parallel to R , and after a linear expansion of terms such as $\exp[iQu(R)]$, we can write the scattering cross section $(d\sigma/d\Omega)_{\text{dis}}$ per D atom for a powder sample as [15, 16]

$$\left(\frac{d\sigma}{d\Omega}\right)_{\text{dis}} = \frac{\sigma_{\text{coh}}}{4\pi} e^{-2W(Q)} \left\{ \sum_{j=1}^{\infty} N_j c_j \frac{2(1-c)u(R_j)}{R_j} \left(\cos(QR_j) - \frac{\sin(QR_j)}{QR_j} \right) \right\}. \quad (5)$$

The factor $1 - c$ in equation (5) arises because the D displacements are defined in comparison to a hypothetical situation in which each interstitial site is occupied by the fraction of a D atom. This situation implies that the average lattice parameter is identical to that of the real system whereas, at the same time, static displacements of the D atoms do not exist. The factor $1 - c$ means further that $(d\sigma/d\Omega)_{\text{dis}}$ becomes zero for the case $c = 1$ in which D displacements do not exist since all interstitial sites are occupied. We see finally that $(d\sigma/d\Omega)_{\text{dis}}$ can be calculated from equation (5) for a given set of the correlation probabilities c_j .

4.3. Incoherent elastic scattering

The scattering cross section $(d\sigma/d\Omega)_{\text{inc}}$ per D atom from the incoherent elastic scattering processes is given by

$$\left(\frac{d\sigma}{d\Omega}\right)_{\text{inc}} = \frac{\sigma_{\text{inc}}}{4\pi} e^{-2W(Q)} \quad (6)$$

where $\sigma_{\text{inc}} = 2.05 \text{ b}$ is the incoherent scattering cross section of the D atoms [17].

4.4. Coherent and incoherent inelastic scattering from the optic D vibrations

H interstitials in BCC metals such as V, Nb and Ta metals perform high-frequency optic vibrations (local modes) with energies that are practically independent of the wave vector, even for high H concentrations [27]. In those cases in which more than one H isotope was investigated, the ratio of the vibrational energies of the H and the D scaled closely to the

root of the respective inverse mass [27]. We do not know of any experiments investigating the optic D vibrations in cubic VD_x . For this reason, we assume that the energies of the D vibrations are a factor of $\sqrt{2}$ smaller than those measured for the isotope H. This yields the energies $\hbar\omega_1 \simeq 80$ meV and $\hbar\omega_2 = \hbar\omega_3 \simeq 120$ meV for the three optic vibrations of a D atom ($\hbar\omega_2$ and $\hbar\omega_3$ are degenerate for symmetry reasons) [27, 28].

For the calculation of the scattering cross section $(d\sigma/d\Omega)_{opt}$ per D atom due to its three optic vibrations, we have to consider that the energy of the incident neutrons (44.94 meV) is too low for an excitation of the optic modes. Considering further that the energies of the optic vibrations are independent of the wave vector, we can write [29]

$$\left(\frac{d\sigma}{d\Omega}\right)_{opt} = \frac{\sigma_{coh} + \sigma_{inc}}{4\pi} \frac{k_{f,-1}}{k_i} \frac{\hbar Q^2}{2m_D} e^{-2W(Q)} \frac{1}{3} \sum_{j=1}^3 \frac{1}{\exp(\hbar\omega_j/k_B T) - 1} \frac{1}{\omega_j} \quad (7)$$

where $k_B T$ is the thermal energy and m_D is the mass of a D atom. The wave vector $k_{f,-1}$ of the inelastically scattered neutrons is given by

$$k_{f,-1} = \sqrt{k_i^2 + \frac{2m_N\omega_j}{\hbar}} \quad (8)$$

where m_N is the mass of a neutron. The scattering angle 2Θ , finally, is defined according to equation (2) where k_f has to be replaced by $k_{f,-1}$.

4.5. Coherent and incoherent inelastic scattering from the acoustic D vibrations

H interstitials in metal-H systems modify the acoustic vibrations of the metal only slightly. However, they participate in the acoustic vibrations, which causes the so-called band modes of the H [27, 30–32]. For the band modes, the vibrational amplitudes of the H are similar to those of the host metal, although they are not completely identical [31]. In the present situation, the band modes of the D lead to inelastic scattering processes whose intensity, per D atom, will be described by the scattering cross section $(d\sigma/d\Omega)_{band}$. Under consideration of the fact that experimental data for the band modes of the VD_x system are not available, we shall assume that the vibrational amplitudes of the D atoms are indeed identical to those of the V host metals. We shall further neglect the dispersion properties of the band modes, so that the scattering cross section can be written as [29]

$$\left(\frac{d\sigma}{d\Omega}\right)_{band} = \frac{\sigma_{coh} + \sigma_{inc}}{4\pi} \frac{\hbar Q^2}{2m_V} e^{-2W(Q)} \times \int d\omega \frac{Z(\omega)}{\omega} \left\{ \frac{k_{f,-1}}{k_i} \frac{1}{\exp(\hbar\omega/k_B T) - 1} + \frac{k_{f,+1}}{k_i} \frac{\exp(\hbar\omega/k_B T)}{\exp(\hbar\omega/k_B T) - 1} \right\} \quad (9)$$

where m_V is the mass of a V atom and $k_{f,-1}$ or $k_{f,+1}$ are the wave vectors of the scattered neutron after a phonon annihilation or creation process, respectively. The wave vectors are given by the equation

$$k_{f,\mp 1} = \sqrt{k_i^2 \pm \frac{2m_N\omega}{\hbar}}. \quad (10)$$

The scattering angle 2Θ is again defined by equation (2) where k_f has to be replaced by $k_{f,-1}$ or $k_{f,+1}$, respectively. The quantity $Z(\omega)$ is the phonon density of states of the V host lattice, normalized to unity. In our numerical calculation of $(d\sigma/d\Omega)_{band}$, we used for $Z(\omega)$ the experimental values given in [33]. We repeat that the contribution of $(d\sigma/d\Omega)_{band}$ to the total scattering cross section will be found to be very small, a fact that justifies the simplifying assumptions leading to equation (9).

4.6. Debye–Waller factor

In calculating the Debye–Waller factor $e^{-2W(Q)}$, we have to consider both the contribution from the optic modes and that from the acoustic band modes. Accordingly, we can write

$$2W(Q) = \frac{1}{3} Q^2 (\langle u_{\text{opt}}^2 \rangle + \langle u_{\text{band}}^2 \rangle) \quad (11)$$

where $\langle u_{\text{opt}}^2 \rangle$ and $\langle u_{\text{band}}^2 \rangle$ are the expectation values for the vibrational amplitude of a given D atom resulting from the optic and band modes, respectively. At room temperature, the energies of the optic vibrations as given in section 4.4 yield $\langle u_{\text{opt}}^2 \rangle = 0.031 \text{ \AA}^2$, whereas $\langle u_{\text{band}}^2 \rangle$ is found to be 0.018 \AA^2 [34], again assuming that the vibrational amplitudes of D are identical to those of the V atoms. These values agree essentially with those stated in [31] if we account for the fact that the data there were taken for the isotope H.

5. Analysis of the experimental data and discussion

With the help of the above expressions for the individual scattering cross sections, we performed numerical calculations for the diffuse scattering intensity in figure 2. The unknown parameters were the correlation probabilities c_j and a normalization factor that was identical for all the scattering cross sections. In our calculations, we considered short-range order effects for the D atoms up to the fifteenth shell of tetrahedral sites. This means that the correlation probabilities c_j could differ from c for $j \leq 15$, whereas they were identical to c for $j > 15$, so that the summation in equation (1) extended only over the first fifteen shells. A further simplification was that, for $8 \leq j \leq 15$, all the c_j were assumed to be identical.

For the scattering cross section from the static displacements of the D atoms, given in equation (5), we considered in our summation 1000 shells. This turned out to be sufficient since parallel calculations with a much smaller number of shells (usually 100) yielded practically the same result within the relevant range of scattering angles 2Θ . For the calculation of the scattering cross section from the acoustic band modes, the integration over the phonon density of states $Z(\omega)$ in equation (9) was replaced by a summation over 76 individual terms.

The result of our fitting calculations for the diffuse scattering intensity is indicated by the solid line in figure 2. Within experimental accuracy, the result corresponds to a situation in which a D atom blocks completely the interstitial sites in the first and the second shell ($c_1 = c_2 = 0.00 + 0.02 / -0.00$). The calculation yielded further $c_3 = 0.09 \pm 0.01$, $c_4 = 0.14 \pm 0.04$, $c_5 = 0.17 \pm 0.02$ and occupation probabilities c_j for the outer shells 6–15 that differed only slightly from the average value $c = 0.125$. The results for all the c_j , and their confidence limits, are listed in table 1, together with the values of R_j and N_j for the individual shells. The blocking of the two nearest shells demonstrates indeed the existence of a strong and repulsive interaction between the D atoms, as already suggested in previous studies [4, 6, 9–14]. The result for c_3 means further a definite non-zero occupation probability which, however, is smaller than the average $c = 0.125$, corresponding to a partial blocking of the third shell. The large error of c_4 resulting in part from the fact that the number of sites in the fourth shell is smaller than that in its neighbouring shells, does not allow a reliable statement on a deviation from the average occupation probability.

Table 1. Compilation of the correlated occupation probabilities c_j resulting from the fitting calculation for the data in figure 2. The table shows the c_j for the respective shell, the distance R_j between the site in the centre and the sites in the shell and the number N_j of the sites in shell j . The table does not show results for shell 14 since the number of sites in this shell is zero. Note that in our calculation procedure the occupation probabilities c_8 – c_{15} were considered as one single fit parameter.

Number of the shell j	Occupation probability c_j	Distance R_j (Å)	Number of sites N_j
1	0.00+0.02/–0.00	1.122	4
2	0.00+0.02/–0.00	1.587	2
3	0.09±0.01	1.943	8
4	0.14±0.04	2.244	4
5	0.17±0.02	2.508	8
6	0.15±0.02	2.748	8
7	0.12±0.01	2.968	16
8	0.117±0.001	3.173	6
9	0.117±0.001	3.365	12
10	0.117±0.001	3.548	8
11	0.117±0.001	3.721	8
12	0.117±0.001	3.886	8
13	0.117±0.001	4.045	24
15	0.117±0.001	4.345	16

On the other hand, the occupation probability c_5 for the fifth shell has a value clearly above the average $c = 0.125$.

The broken line in figure 2 is the sum of the diffuse scattering intensities resulting from the displacements of the D atoms, the incoherent elastic scattering and from both the optic and the acoustic phonons. It is these contributions to the total scattering intensity whose calculation according to equation (5), (7) and (9) involved several simplifying approximations. We show these contributions separately in order to demonstrate that they represent only a minor part of the total scattering intensity. This fact justifies our simplifying assumptions since potential inaccuracies in the calculation of these contributions are not expected to influence seriously the total scattering intensity. It also shows that the scattering intensity from the short-range order of the D atoms, as given in equation (1), represents in fact the dominant contribution to the total scattering intensity.

The present data clearly evidence the presence of a strong and repulsive short-range interaction between the D atoms. In order to demonstrate more clearly the reliability of our results for the three nearest shells around a given D atom, we show the diffuse scattering intensity from the D in $\text{VD}_{0.75}$ again in figure 3 together with model calculations for the scattering intensity (the experimental data in figure 2 and figure 3 are identical). The model calculations were carried out (i) for a complete blocking of the first shell (solid line), (ii) for a complete blocking of the first and the second shell (broken line) and (iii) for a complete blocking of the three nearest shells (dash-dot line). For reasons of simplicity, the occupation probabilities of the outer shells were assumed to be identical to c . The calculated intensities show that a complete (or a nearly complete) blocking of the first two shells seems indeed to be required for a theoretical description of the data, whereas this description is obviously not improved by the additional assumption of a complete blocking of the third shell. These considerations indicate again a nearly complete blocking of the first two shells and a partial blocking of the third shell, as already concluded from the result of our fitting calculation as shown in figure 2.

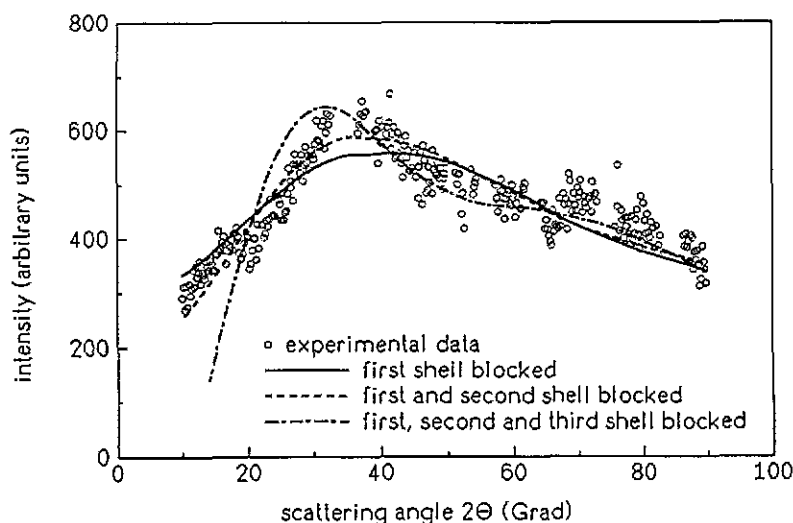


Figure 3. Diffuse scattering intensity of the D atoms in $\text{VD}_{0.75}$ together with model calculations for the scattering intensity (the experimental data are identical to those of figure 2). The model calculations were carried out for (i) a complete blocking of the first shell (full line), (ii) a complete blocking of the first and second shells (broken line) and (iii) a complete blocking of the first three shells (dash-dot line). For reasons of simplicity, the occupation probabilities of all the outer shells were assumed to be identical to $c = 0.125$.

6. Conclusion

The short-range order of D atoms in $\text{VD}_{0.75}$ was investigated by neutron diffraction. The diffuse scattering intensity can be described by a nearly complete blocking of the interstitial sites in the two nearest shells around a given D atom, and by a reduced occupation probability for the sites of the third shell. These results demonstrate the existence of a strong short-range and repulsive interaction between the D atoms.

Acknowledgment

The present work was supported by the Bundesministerium für Forschung und Technologie.

References

- [1] Schober T and Wenzl H 1978 *Hydrogen in Metals II (Topics in Applied Physics 29)* ed G Alefeld and J Völkl (Berlin: Springer) p 11
- [2] Wicke E, Brodowsky H and Züchner H 1978 *Hydrogen in Metals II (Topics in Applied Physics 29)* ed G Alefeld and J Völkl (Berlin: Springer) p 73
- [3] Fukai Y and Sugimoto H 1985 *Adv. Phys.* **34** 263
- [4] Switendick A C 1979 *Z. Phys. Chem., NF* **117** 89
- [5] Mokrani A and Demangeat C 1989 *Z. Phys. Chem., NF* **163** 541
- [6] Westlake D G 1983 *J. Less Common Metals* **91** 1
- [7] Veleckis E and Edwards R K 1969 *J. Phys. Chem.* **73** 683
- [8] Rummel W 1981 *Siemens Forsch.-Entwickl.-Ber.* **10** 371

- [9] Wagner H 1978 *Hydrogen in Metals I (Topics in Applied Physics 28)* ed G Alefeld and J Völkl (Berlin: Springer) p 5
- [10] Boureau G 1984 *J. Phys. Chem. Solids* **45** 973
- [11] Sotzek M, Siebler H, Wipf H and Leuthäusser U 1984 *J. Less Common Metals* **104** 21
- [12] Shirley A I and Hall C K 1986 *Phys. Rev. B* **33** 8084, 8099
- [13] Meuffels P and Oates W A 1987 *J. Less Common Metals* **130** 403
- [14] Hempelmann R, Richter D, Faux D A and Ross D K 1988 *Z. Phys. Chem., NF* **159** 175
- [15] Krivoglaz M A 1969 *Theory of X-Ray and Thermal-Neutron Scattering by Real Crystals* (New York: Plenum)
- [16] Warren B E 1969 *X-Ray Diffraction* (Reading, MA: Addison-Wesley)
- [17] Sears V F 1992 *Neutron News* **3** 27
- [18] Magerl A, Zabel H and Wipf H 1984 *J. Less Common Metals* **103** 91
- [19] Blech I A and Averbach B L 1965 *Phys. Rev. A* **137** 1113
- [20] Blank H and Maier B (eds) 1988 *The Yellow Book, Guide to Neutron Research Facilities at the ILL*
- [21] Peisl H 1973 *Hydrogen in Metals I (Topics in Applied Physics 28)* ed G Alefeld and J Völkl (Berlin: Springer) p 53
- [22] Dederichs P H 1973 *J. Phys. F: Met. Phys.* **3** 471
- [23] Metzger T H, Behr H, Steyrer G and Peisl J 1983 *Phys. Rev. Lett.* **50** 843
- [24] Dosch H, Peisl J and Dorner B 1987 *Phys. Rev. B* **35** 3069
- [25] Leibfried G and Breuer N 1978 *Point Defects in Metals I* (Berlin: Springer)
- [26] Magerl A, Berre B and Alefeld G 1976 *Phys. Status Solidi a* **36** 161
- [27] Springer T 1978 *Hydrogen in Metals I (Topics in Applied Physics 28)* ed G Alefeld and J Völkl (Berlin: Springer) p 75
- [28] Magerl A, Rush J J and Rowe J M 1986 *Phys. Rev. B* **33** 2093
- [29] Lovesey S W 1984 *Theory of Neutron Scattering from Condensed Matter* vol 1 (Oxford: Clarendon)
- [30] Kley W 1966 *Z. Naturf. Suppl. a* **21** 1770
- [31] Lottner V, Heim A and Springer T 1979 *Z. Phys. B* **32** 157
- [32] Lottner V, Schober H R and Fitzgerald W J 1979 *J. Phys. Rev. Lett.* **42** 1162
- [33] Landolt-Börnstein 1981 *New Series* vol 13a, ed P H Dederichs, H Schober and D J Sellmyer (Berlin: Springer) p 163
- [34] Kamal M, Malik S S and Rorer D 1978 *Phys. Rev. B* **18** 1609